Available online at www.sciencedirect.com

ScienceDirect

Procedia Computer Science 112 (2017) 980–988

Procedia Computer Science

www.elsevier.com/locate/procedia

International Conference on Knowledge Based and Intelligent Information and Engineering Systems, KES2017, 6-8 September 2017, Marseille, France

Automatic vessel detection by means of brightness profile characterization in OCT images

Joaquim de Moura[a*], Jorge Novo[a], José Rouco[a], Manuel G. Penedo[a], Marcos Ortega[a]

[a] *University of A Coruña - Department of Computing, Campus de Elvia S/N, A Coruña - 15071, Spain*

Abstract

Optical Coherence Tomography (OCT) is a well-established medical imaging technique that allows the analysis of the eye fundus characteristics in real time. These images enable the experts to make a clinical evaluation of the retinal vasculature, whose morphology provides relevant information for diseases like diabetes, hypertension or arteriosclerosis. In this paper, we present a novel proposal for the automatic vasculature identification in retinal OCT images. To achieve this, we analyse the intensity profiles between representative retinal layers, previously segmented. Then, two statistical models are generated using representative samples of vessel and non-vessel profiles. The analysis of both statistical models let us optimize the discrimination of both cathegories that is used, finally, to identify the vessel locations. The proposed method was adjusted and validated using 256 OCT images, including 1274 vascular structures that were labelled by an expert clinician. Satisfactory results were provided as a precision of 94.55% and a recall of 90.25% were obtained, respectively. The method facilitates the doctors' work allowing better analysis and treatments of vascular diseases.

Peer-review under responsibility of KES International

Keywords: Computer-aided diagnosis; retinal imaging; Optical Coherence Tomography; vessel detection

1. Introduction

The retinal vasculature is a complex structure whose analysis can provide potential biomarkers for diseases like diabetes, hypertension or arteriosclerosis[1 2 3]. Optical coherence tomography (OCT) is a noninvasive high-resolution optical imaging technique that provides histological tomographical images of the eye fundus[4]. This method allows the capture of images of the retinal tissues that include the presence of the retinal vasculature[5], enabling the experts to make accurate analysis and clinical evaluations. In these images, the retinal vessels are visualized as structures that block the transmission of light and leave a shadow, as illustrated in Fig. 1.

* Corresponding author. Tel.: +34-881011330 ; fax: +34-981167160.
E-mail address: joaquim.demoura@udc.es

1877-0509 © 2017 The Authors. Published by Elsevier B.V.
Peer-review under responsibility of KES International
10.1016/j.procs.2017.08.142

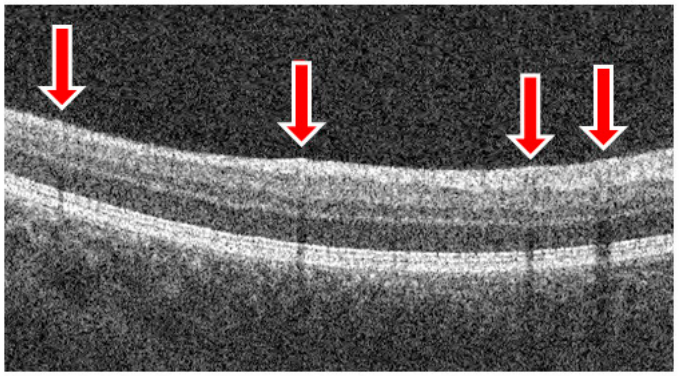

Fig. 1. OCT histological image with the shadow projections of a set of vessels.

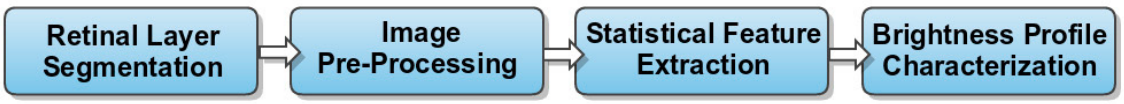

Fig. 2. Main steps of the proposed methodology.

In the state of the art, we can find many different approaches that faced this problem in classical retinographies. As reference, Nekovei *et al.*[6] based his proposal on the application of neural networks using a back-propagation algorithm with the momentum term. In the case of Elbalaoui *et al.*[7], a Hessian multiscale enhancement filter is designed from an adaptive thresholding for vessel detection. Espona *et al.*[8] proposed a methodology based on the use of deformable contour models, incorporating domain specific knowledge such as topological properties of the blood vessels to identify them.

However, few studies were proposed using OCT images. Moreover, the proposals used, as support, the corresponding near-infrared reflectance retinography for the vascular detection process. Niemeijer *et al.*[9] used a 2D projection of the vessel pattern to obtain a high contrast between the vessel silhouettes and the retinal background. Guimarães *et al.*[10] employed the OCT fundus images to locate the depth of the vessels, enclosed in the study of abnormal retinal vascular patterns. Moura *et al.*[11] detected the vasculature in the retinography and projected these 2D locations in the OCT histological images to estimate the depths along all the vessel tree.

We propose, in this work, a novel and complete methodology for the automatic detection of retinal vessels using, only, the OCT histological images. The method segments the retinal layers and detects the vessel structures by the analysis of vessel and non-vessel profiles obtained between these layers. Using this analysis, statistical models are constructed for both categories that are used to determine the vessel identifications.

2. Methodology

The proposed methodology is divided into four main steps: firstly, the retinal layers are segmented using the input image; secondly a preprocessing is applied to enhance the characteristics of the vascular structures; then, a set of statistical features is extracted, modelling the brightness profiles of both categories; finally, the vessels are detected using these profile characterizations. A schematic representation of the main steps of this methodology can be seen in Fig. 2.

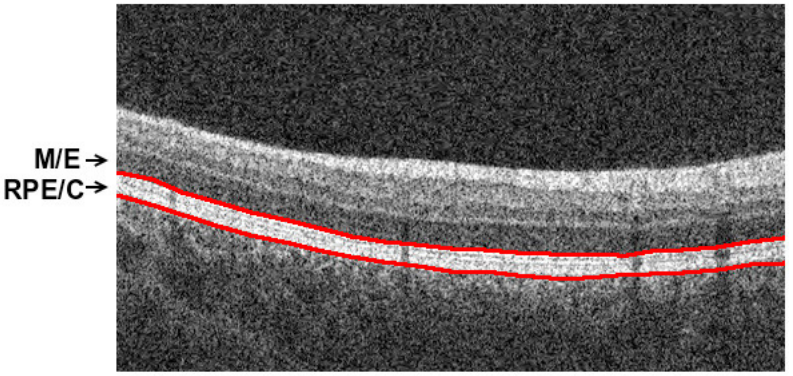

Fig. 3. Example of (M/E) and (RPE/C) retinal layer segmentation.

2.1. Retinal Layer Segmentation

The OCT image represents the morphology of the retina with sufficient histological quality to appreciate the vascular structures and their respective shadows that are projected on the layers of the retina. The vascular shade is most prominent in the region between the following retinal layers: Pigment Epithelium Bruch's Complex with the Choroid (RPE/C) and top boundaries of the Ellipsoid (M/E). The first step of the methodology consists of restricting the search region to the area between these retinal layers. To achieve this, we use the methodology proposed in [12], where the retinal layers are segmented using snakes, an active contour-based approach. This method defines each retinal layer as a polygonal surface that, placed in the image, evolves until it reaches the optimal adjustment with the shape of the aimed structure. Each vertex of the snake is moved according to inner and outer forces, and the general contour becomes stable when the minimum of the energy function is achieved. These energy forces are measured by the energy function ξ_{snake} (Eq. 1), where ξ_{int} represents the internal energy (the snake flexibility and elasticity), and ξ_{ext} the external energy (the forces that push the snake towards the edges of the shape).

$$\xi_{snake}(s) = \int \xi_{int}(s)ds + \int \xi_{ext}(s)ds \tag{1}$$

In Fig. 3, we can see a representative example of the result of this segmentation stage, identifying the region of interest that is used in the following phases.

2.2. Image Pre-Processing

OCT images are characterized by the presence of a granular pattern known as speckle noise that complicates the process of identification and interpretation of retinal structures. For that reason, a noise reduction and contrast enhancement is desirable in the analysed regions. To achieve that, a Gaussian blur filter is applied to reduce this speckle noise in the image. Then, a top-hat transform is used vertically to increase the contrast of the vascular shadows. Fig. 4 illustrates the results that are obtained in this step of the methodology.

2.3. Statistical Feature Extraction

In this phase, we calculate the statistical characteristics that are posteriorly used in the construction of the models that represent the vessel and non-vessel profiles. Three statistical features are calculated within the region of interest that is delimited by the layers (RPE/C) and (M/E) of the pre-processed image:

- m_i: median of the intensity profiles in each column c_i.
- μ_i: mean of the intensity profiles in each column c_i.

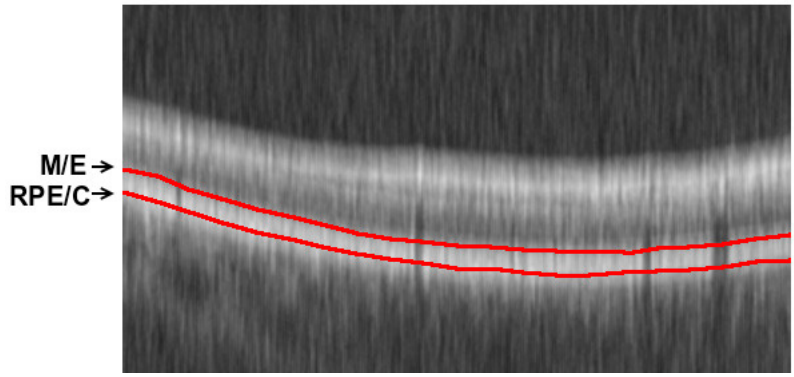

Fig. 4. Example of pre-processed image after noise removal and contrast enhancement.

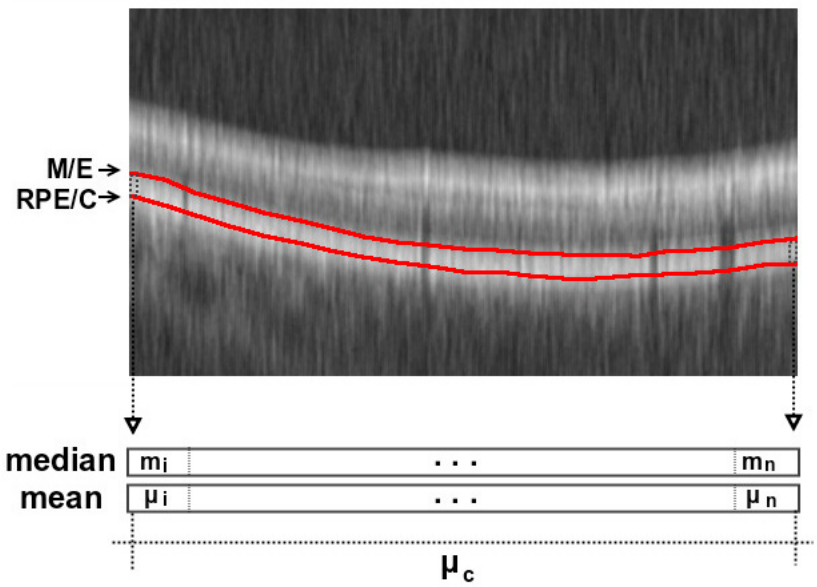

Fig. 5. Statistical feature (m_i, μ_i and μ_c), extraction process.

- $\mu_i - \mu_c$: mean μ_i of the intensity profiles in each column c_i minus the mean μ_c calculated for each OCT histological image c.

Fig. 5, shows a representation of the statistical feature calculation (m_i, μ_i and μ_c) in an OCT image.

2.4. Brightness Profile Characterization

The defined statistical features were calculated in a set of OCT images. This information was used to analyse the brightness profile characterization and identify the vessel and non-vessel profiles. Histograms of both classes are, then, calculated, obtaining the models for both categories. These brightness profile models are used to determine the optimal threshold, *th*, that is used to separate both classes in the histogram. Fig. 6 illustrates the representation of the models for vessels and non-vessels, identifying the parts that belongs to: True Positive (TP), False Positive (FP), True Negative (TN) and False Negative (FN). The optimal threshold, *th*, is obtained through the analysis of the following measurements: precision, recall and f-score (Eqs. (2), (3) & (4), respectively). Hence, *th* is the value that represents

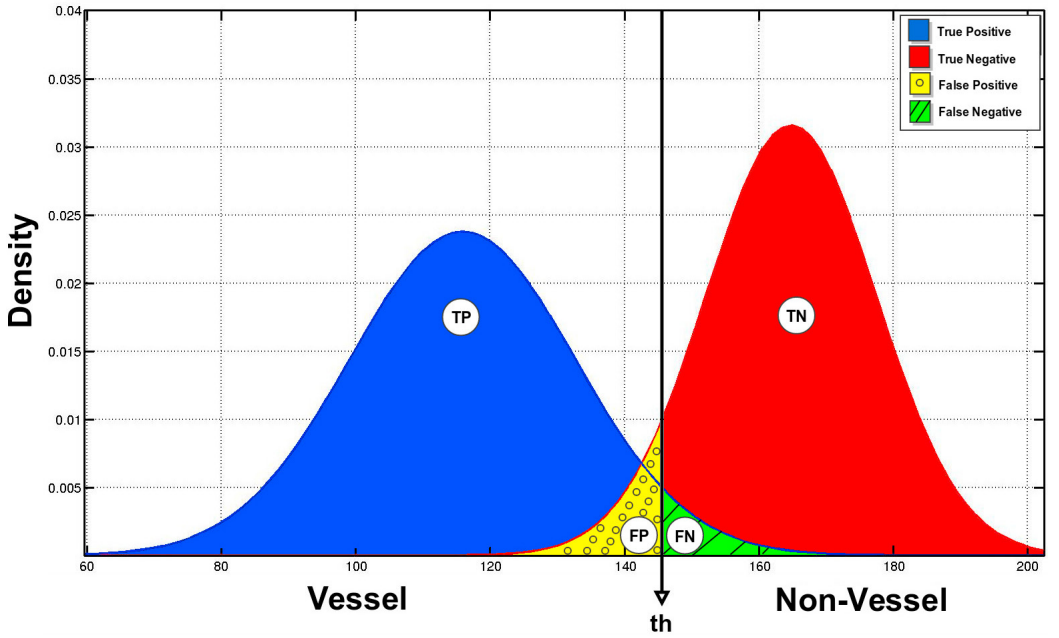

Fig. 6. Models for vessel and non-vessel profiles using: TP, FP, TN and FN. The optimal threshold, *th*, represents the value that separates the histogram into two classes: Vessel and Non-Vessel.

the best compromise between precision and recall identified by the maximum f-score value that is calculated for each feature.

$$Precision = \frac{TP}{TP + FP} \tag{2}$$

$$Recall = \frac{TP}{TP + FN} \tag{3}$$

$$F - Score = 2 \cdot \left(\frac{Precision \cdot Recall}{Precision + Recall} \right) \tag{4}$$

Once the optimal threshold is applied, the detected columns are grouped by connectivity. The final vessel detections are determined by the central point of each group.

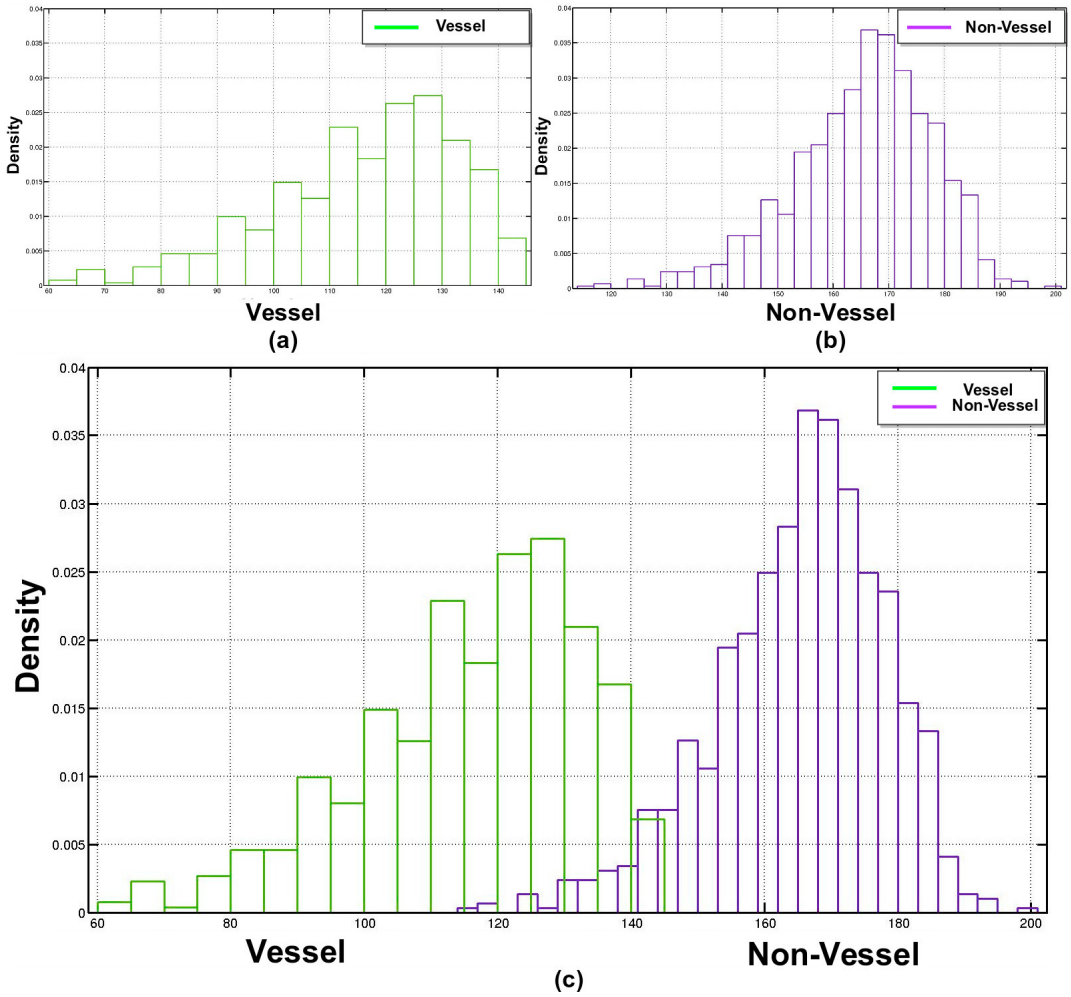

Fig. 7. Histograms representing the mean brightness profiles, μ_i, using the training dataset. (a) Vessel profile. (b) Non-Vessel profile. (c) Vessel and Non-Vessel profiles.

3. Experimental Results

The proposed method was tested using 256 OCT histological images. These images were taken with a confocal scanning laser ophthalmoscope, CIRRUS^{TM} HD-OCT Carl Zeiss, with Spectral Domain Technology, at a resolution of 490×500 pixels. These images are centered on the macula, from both left and right eyes of different patients. A total of 1274 vessels have been manually labelled by an expert clinician. We randomly divided the dataset into a training and a testing dataset, both including 128 images.

Regarding the training dataset, it contained 1502 profiles, 525 coming from vessels and 977 selected from non-vessel profiles. Fig. 7, shows the vessel and non-vessel histograms that were obtained using the statistical feature μ_i.

The optimal threshold, th, was identified, as said, by the evaluation of the accuracy of the proposed method using three measurements: precision, recall and f-score. Table 1 summarizes the results of the optimal threshold, th, obtained using each feature. In Fig. 8, we can see the ROC curve, using precision and recall, with the results for each of the analysed features: m_i, μ_i and $\mu_i - \mu_c$.

Table 1. Precision, Recall and F-Score in the calculation of the optimal threshold, *th*.

Feature	th	Precision	Recall	F-Score
m_i	136	89.3651%	88.3695%	0.888645
μ_i	131	91.0356%	90.2545%	0.906433
$\mu_i - \mu_c$	-30	92.5696%	91.5475%	0.920557

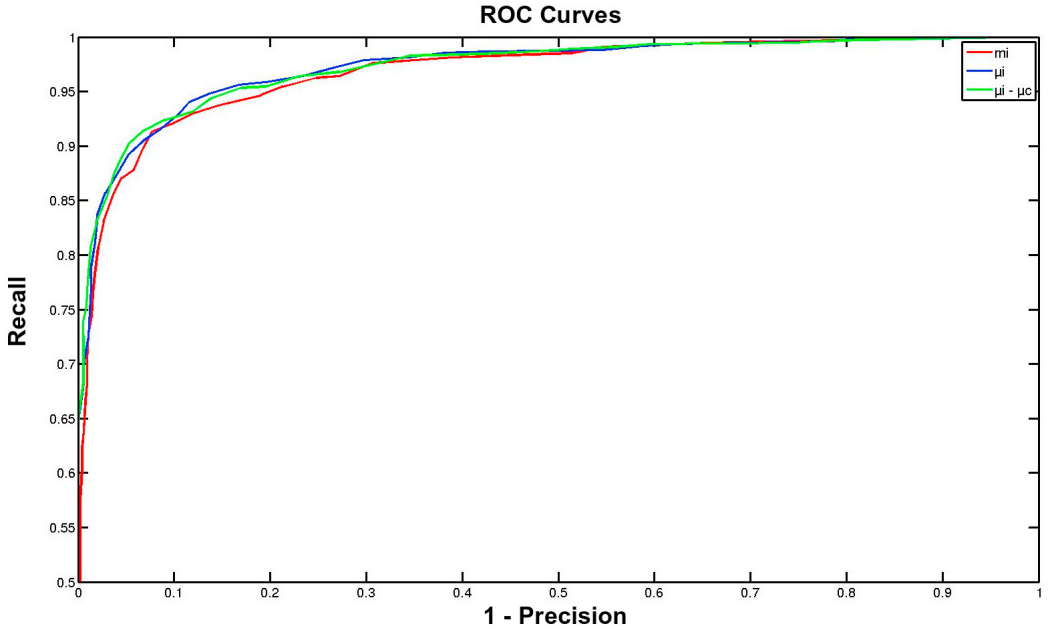

Fig. 8. ROC curves with the results of the used features: m_i, μ_i and $\mu_i - \mu_c$.

Regarding the validation phase, the testing dataset was composed by 749 vessel and 839 non-vessel profiles. Table 2 presents the results that were obtained using each statistical feature. Although there is no great differences among them, both in training and testing stages the $\mu_i - \mu_c$ was the feature that offered a better and more complete performance to the vessel detection process, with a f-score of 92.34%. The best performance of $\mu_i - \mu_c$ derives from the fact that it normalizes the mean of the column by the global mean of the image, making that this feature is more robust to the parameters of brightness and contrast that may vary during the image acquisition, situation that is common in this type of images.

Table 2. Precision, Recall and F-Score results using the testing dataset.

Feature	Precision	Recall	F-Score
m_i	92.0485%	91.1882%	0.916163
μ_i	94.6175%	89.1855%	0.918213
$\mu_i - \mu_c$	94.5454%	90.2536%	0.923497

Fig. 9 shows representative examples illustrating the results of the proposed method. As we can see, the method is capable to detect vessels of different sizes. We also show a couple of representative errors. Most of the FPs, as happens in Fig. 9(c), are due to shadows that are generated by the presence of other structures that can be present in the retina. Regarding FNs, as the case of Fig. 9(d), they usually appear with small vessels. These vessels produce reduced projected shadows that are more sensitive to alterations produced by noise artefacts that may be introduced during the image capture procedure.

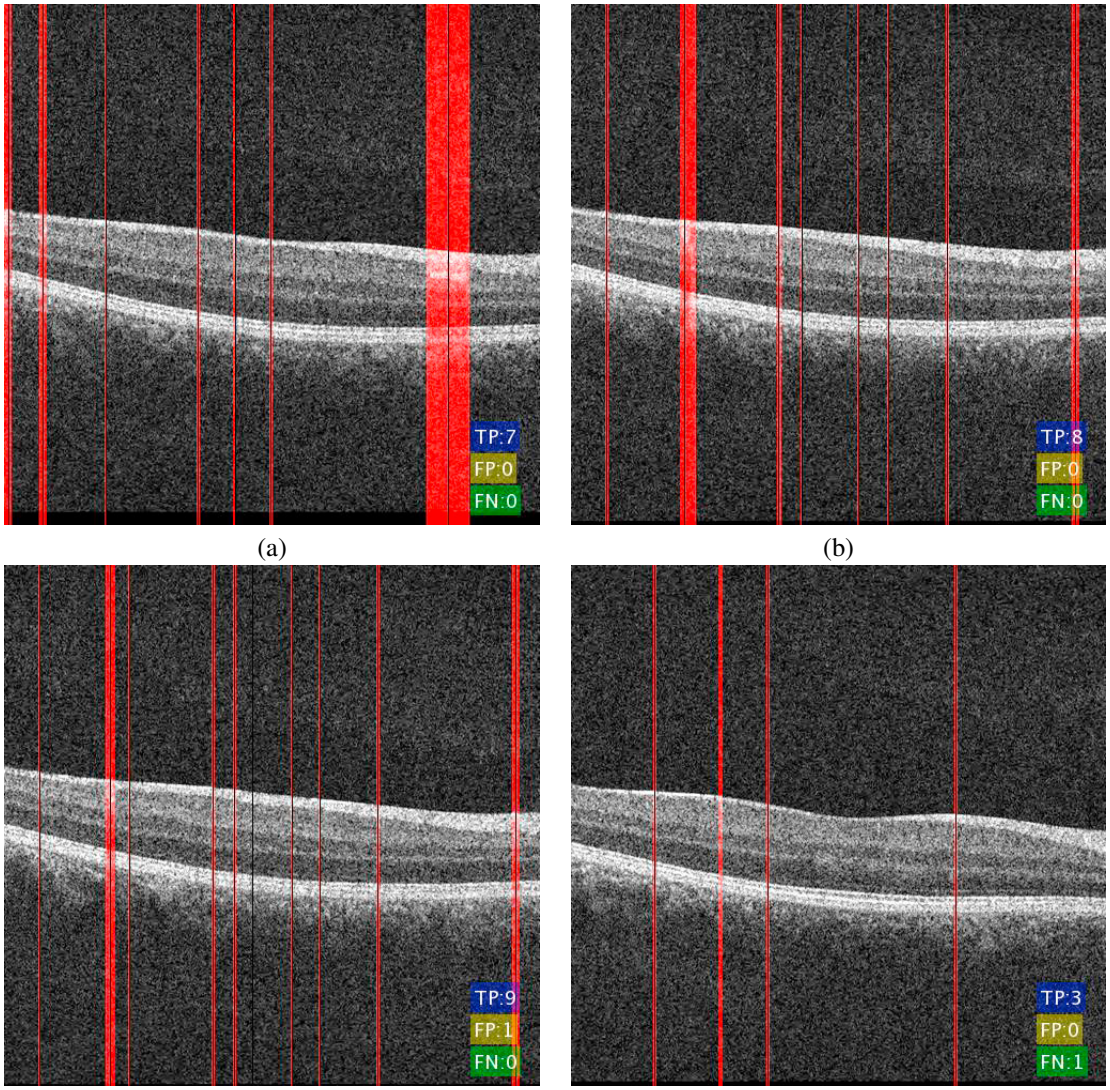

Fig. 9. Examples of results of the proposed method.

4. Discussion and Conclusions

In this paper, we present a new methodology for the automatic vasculature identification in OCT images. The proposed methodology exploits differents statistical features over the brightness profile of the columns between the retinal layers, (RPE/C) and (M/E), to detect the vessels. We used OCT histological images labelled by an expert clinician to construct both vessel and non-vessel profile sets and stablish a discriminant criterion to identify the vessel locations.

We evaluated the robustness and accuracy of the proposed methodology, obtaining accurate results. Analysing the training and testing results of the experiments (see Tables 1 and 2), we can conclude that $\mu_i - \mu_c$ offers a better and more complete performance in the vessel detection process, although it is not observed significant differences with respect to the other features. This automatic vessel identification facilitates the work of the ophthalmologists in diagnostic processes, helping to achieve better analysis and treatments of vascular diseases that are studied in

the retinal microcirculation. As future work, we will study further statistical features that may incorporate higher discriminant power in the vessel identification. Moreover, we want to extend the methodology with the incorporation of the vessel segmentations. Additionally, further analysis with larger image datasets should be done in order to reinforce the conclusions of this work.

Acknowledgements

This work is supported by the Instituto de Salud Carlos III, Government of Spain and FEDER funds of the European Union through the PI14/02161 and the DTS15/00153 research projects and by the Ministerio de Economía y Competitividad, Government of Spain through the DPI2015-69948-R research project.

References

1. Klein R, Sharrett AR, Klein BE, Chambless LE, Cooper LS, Hubbard LD, Evans G. Are retinal arteriolar abnormalities related to atherosclerosis? *Arteriosclerosis, Thrombosis, and Vascular Biology.* 2000 Jun 1;20(6):1644-50.
2. Neubauer AS, Luedtke M, Haritoglou C, Priglinger S, Kampik A. *Retinal vessel analysis reproducibility in assessing cardiovascular disease.* Optometry and Vision Science. 2008 Apr 1;85(4):E247-54.
3. Nguyen TT, Wong TY. Retinal vascular changes and diabetic retinopathy. *Current diabetes reports.* 2009 Aug 1;9(4):277-83.
4. Fercher AF, Drexler W, Hitzenberger CK, Lasser T. Optical Coherence Tomography-principles and applications. *Reports on progress in physics.* 2003 Jan 20;66(2):239.
5. Guedes V, Schuman JS, Hertzmark E, Wollstein G, Correnti A, Mancini R, Lederer D, Voskanian S, Velazquez L, Pakter HM, Pedut-Kloizman T. Optical Coherence Tomography measurement of macular and nerve fiber layer thickness in normal and glaucomatous human eyes. *Ophthalmology.* 2003 Jan 31;110(1):177-89.
6. Nekovei R, Sun Y. Back-propagation network and its configuration for blood vessel detection in angiograms. *IEEE Transactions on Neural Networks.* 1995 Jan;6(1):64-72.
7. Elbalaoui A, Fakir M, Taifi K, Merbouha A. Automatic Detection of Blood Vessel in Retinal Images. *IEEE 13th International Conference InComputer Graphics, Imaging and Visualization (CGiV).* 2016 Mar 29;324-332.
8. Espona L, Carreira MJ, Penedo MG, Ortega M. Retinal vessel tree segmentation using a deformable contour model. *IEEE 19th International Conference InPattern Recognition (ICPR).* 2008 Dec 8;1-4.
9. Niemeijer M, Garvin MK, van Ginneken B, Sonka M, Abramoff MD. Vessel segmentation in 3D spectral OCT scans of the retina. *International Society for Optics and Photonics InMedical Imaging.* 2008 Mar 6;69141R:69141R.
10. Guimarães P, Rodrigues P, Lobo C, Leal S, Figueira J, Serranho P, Bernardes R. Ocular fundus reference images from Optical Coherence Tomography. *Computerized Medical Imaging and Graphics.* 2014 Jul 31;38(5):381-9.
11. de Moura J, Novo J, Ortega M, Barreira N, Penedo MG. Vessel Tree Extraction and Depth Estimation with OCT Images. *InConference of the Spanish Association for Artificial Intelligence.* 2016 Sep 14;23:33.
12. Ortega M, López AG, Penedo MG, Cardeñoso PC. Implementation and Optimization of a Method for Retinal Layer Extraction and Reconstruction in Optical Coherence Tomography Images. *Medical Applications of Artificial Intelligence.* 2013 Nov 6:175.